Water Air Soil Pollut (2014) 225:2028
DOI 10.1007/s11270-014-2028-4

Arsenic Removal from Water by Sugarcane Bagasse: An Application of Response Surface Methodology (RSM)

Hamid Tajernia · Taghi Ebadi · Bahram Nasernejad · Maryam Ghafori

Received: 17 February 2014 / Accepted: 5 June 2014 / Published online: 27 June 2014

Abstract Adsorption is one of the best methods for arsenic removal from water which is established in the last few decades. Biosorption by natural biosorbents and agricultural by-product is an environmental friendly approach and has proved to be a cost-effective and non-hazardous technology for the removal of heavy metals from water. This paper describes batch test findings conducted to evaluate the feasibility of using sugarcane bagasse (SCB) as an industrial by-product of sugar industry to remove arsenic (As) from water and compare the results with the efficiency of activated carbon (AC) for arsenic (As) removal. The effects of three parameters, such as pH, adsorbent dosage (C_a), and initial metal concentration (C_0) on the adsorption of arsenic were evaluated by using response surface methodology (RSM). It is discovered that AC and SCB removed up to ~89 and ~98 % of arsenic, respectively. The uptake capacities yielded from the batch experiment were about 31.25 mg/g for AC at pH ~7.4 and 11.9 mg/g for SCB at pH ~9. The equilibrium times achieved were 120 and 150 min for SCB and AC, respectively. This study shows that SCB is an efficient low-cost biosorption for arsenic removal from water.

Keyword Arsenic removal · Activated carbon · Sugarcane bagasse · Adsorption · Response surface methodology (RSM)

H. Tajernia · T. Ebadi
Department of Civil and Environment Engineering, Amirkabir University of Technology, Tehran, Iran

H. Tajernia
e-mail: hamid.tajernia@aut.ac.ir

B. Nasernejad (✉) · M. Ghafori
Department of Chemical Engineering, Amirkabir University of Technology, Tehran, Iran
e-mail: banana@aut.ac.ir

1 Introduction

Groundwater is the main water resource for human societies. Nearly 60 % of the annual water supply comes out of groundwater sources. Arsenic contaminations of groundwater and surface water have been reported in many parts of the world, for example Bangladesh, India, Argentina, Taiwan, New Zealand, Canada, America, China, Japan, Chile, etc. (Mohan and Pitmann 2007). Inorganic arsenic leads to phenomena such as kidney, bladder, skin, and respiratory tract cancer. Effects of arsenic exposure include as follows: irritation of the stomach and intestines, heart failure, high blood pressure, decreased production of red and white blood cells, damage to DNA, and changes to the skin pigmentation (Lee 2010).

Arsenic and respiratory cancer association studies have proven. Therefore, the International Agency for Research on Cancer (IARC) has categorized arsenic in drinking water in the first group which means that it causes cancer of the respiratory system. The condition of aquatic systems such as oxidation–reduction, precipitation, and ligand exchange changes the chemistry of arsenic in water (Baskan and Pala 2011). Arsenic

compounds such as arsenite, arsenate, arsenic acid, arsenious acid, methyl arsenic acid, and dimethyl arsenic are observed in the environment. Arsenic with +3 and +5 capacities in aquatic environments has been observed. The trivalent arsenic form is more toxic than pentavalent and organic forms (Eljamal et al. 2011). Most of the arsenics have been seen in both redox conditions. Two forms of arsenic commonly found in natural polluted water are arsenate and arsenite. In aerobic and oxidizing conditions, predominant species are pentavalent species and in anaerobic and moderately reducing conditions are trivalent species (Mohan and Pitmann 2007; Maji et al. 2008; Eljamal et al. 2011; Di Natale et al. 2008).

Different methods have been used in arsenic removal such as precipitation, oxidation, ion exchange, adsorption, and ultrafiltration (Pandey et al. 2009). Adsorption is one of the best methods in contaminant removal from water which is established in the last few decades. Activated carbon is an organic sorbent which is commonly used to remove different contaminants from water and has been widely used as an adsorbent. Types of the activation processes can change the functional groups. Because of high surface area and different types of active groups (carboxylic acid, hydroxyl, carbonic, etc.), activated carbon (AC) has high adsorption capacity.

Low-cost adsorbents are used for heavy metal removal because they are less expensive than membrane separation and synthetic materials such as ACs. Biosorption process by natural biosorbents and agricultural by-product is an environmental friendly approach and has been proved to be a cost-effective and non-hazardous technology for the removal of heavy metals from water. Some natural sorption materials such as natural laterite, red mud, modified sawdust, coconut husk carbon, and waste rice husk have been investigated by other researchers (Manju et al. 1998; Urík et al. 2009; Maiti et al. 2009; Amin et al. 2006). Some materials and their maximum arsenite uptake are shown in Table 1.

We choose the raw sugarcane bagasse (SCB) for arsenic removal because no study has been done on the removal of arsenic by raw SCB and treated SCB as biosorbents. Actually, SCB is a low-cost residue (by-product) in sugar industry remaining after the sugar is extracted and contains large quantities of cellulose and lignin. Therefore, regarding the adsorptive sites such as carboxylic, carbonyl, amine, and hydroxyl groups, SCB can adsorb heavy metal ions especially arsenic from water. SCB has been used as a natural adsorbent in the following three main forms: fly ash, activated carbon, and native or raw bagasse for the purposes of separation, determination, or removal of different types of

Table 1 Some adsorbents of arsenic

Absorbent	Arsenite uptake (mg/g)	Reference
AC	29.9	(Mohan and Pitmann 2007)
Orange juice residue	70.43	(Akhter et al. 1997)
Fresh biomass	128.1 (90 %)	(Kamala et al. 2005a, b)
Red mud	0.884 (87 %)	(Altundogan et al. 2002)
Immobilized biomass	7.4	(Mohan and Pitmann 2007)
Tea fungal biomass	1.11	(Murugesan et al. 2006)
AC (olive pulp)	1.39	(Budinova et al. 2006)
Green algae	57.48	(Sari et al. 2011)
Char carbon	89.24	(Pattanayak et al. 2000)
Oxisol	2.6	(Ladeira and Ciminelli 2004)
Gibbsite	3.3	(Ladeira and Ciminelli 2004)
Bean pod AC	13.5	(Budinova et al. 2009)
ZVI-AC	15	(Zhu et al. 2009)
ZVI-sheep manure	30.96	(Wilopo et al. 2008)
Fly ash	74.4	(Polowczyk et al. 2010)
Sugarcane bagasse	11.9	(This study)
AC	31.25	(This study)

pollutants. These include heavy metal ions (Gupta et al. 1998a, 1999; Gupta et al. 2003; Gupta and Ali 2004; Ayyappan et al. 2005; Mohan and Singh 2002; Garg et al. 2008; Rao et al. 2002; Gupta and Ali 2000; Rao et al. 2009), dyes (Srivastava et al. 1995a, b; Gupta et al. 1998b, 2000, 2005; Gupta et al. 2009; Mane et al. 2007) and pesticides (Gupta and Ali 2001; Gupta et al. 2006; Akhtar et al. 2007; Gupta et al. 2003). In case of heavy metal ions, several studies have been conducted towards the separation and removal of one, two, or three metal ions. Bagasse fly ash was used for the removal or uptake of copper and zinc (Gupta and Ali 2000), chromium and nickel (Rao et al. 2002), lead and chromium (Gupta and Ali 2004), and cadmium and nickel (Gupta et al. 2003). Bagasse activated carbon was also used for the removal of Cd (II) and Zn (II) (Mohan and Singh 2002) and Hg (II) (Rao et al. 2009) and Pb (II) (Ayyappan et al. 2005). However, few studies have been directed towards the use of its raw or native form for the purpose of metal ion removal (Garg et al. 2008; Rao et al. 2002).

The objectives of this study are to test and compare AC and SCB as alternative suitable arsenic adsorbents. In this study, we used an experimental design for the optimization of arsenic removal tests by applying Box–Behnken design under response surface methodology (RSM) using Design Expert software (Version 7.0.0, Stat. Ease. Inc., USA), and the experimental data were analyzed with a second-order polynomial model validated by statistical analysis. To specify the surface morphology, a scanning electron microscope (SEM) was applied. Fourier transform infrared (FTIR) analysis was done to identify different functional groups present on the surface of the adsorbent.

2 Materials and Methods

2.1 Materials

All chemicals were of reagent grade. All glassware and sample bottles were washed with a detergent solution, rinsed with tap water, soaked with 10 % nitric acid for at least 12 h, and finally rinsed with distilled water three times. All aqueous solutions were prepared in double-distilled water. Arsenic solutions were made from arsenic trioxide (As_2O_3) and NaOH which were both from Merck Company. Standard arsenite solution (1,000 mg/L) was prepared by dissolving 1.320 g of arsenic trioxide (As_2O_3) in a minimum volume of 20 % NaOH. It was then neutralized with nitric acid and diluted to 1,000 mL (Budinova et al. 2009; Kamala et al. 2005a). The characterizations of AC in this study are shown in Table 2. The particle size of SCB was about 100–850 μm, and its density was about 344 Kg/m^3 with water adsorption about 70–75 %. Table 3 shows the lignocellulosic SCB compositions.

Table 2 The characterizations of AC

AquaCarb®820	Parameter
Bituminous Coal	Type of AC
8*20	Particle size
>1,000	BET, m^2/g
1,000	Iodine no., mg/g

2.2 Biosorbent Preparation

The SCB was boiled for 3 h and then washed several times with double-distilled water to remove impure particles and other soluble components such as coloring agents. Then, it was dried at 80 °C in a convection oven for 24 h (Khoramzadeh et al. 2013a, b).

2.3 Adsorption Procedure

For the experimental design and optimization, response surface methodology (RSM) was employed. The Box–Behnken designed experiment model was used for the design of the required number of experiments. The pH, initial concentration, and adsorbent dosage were considered as effective parameters on adsorption processes. Batch tests designed by RSM were carried out by mixing certain amounts of SCB and AC with 100 mL of aqueous solution in a 250-mL conical flask, the batch tests were conducted at room temperature (24±2 °C) by a mechanical shaker at 180 rpm for 30 min. After filtration, using 0.45-μm filters, remaining arsenic (As) ion concentrations in the solution were analyzed by an atomic adsorption spectrophotometer at a maximum adsorption wavelength (λ_{max}=193.7 nm). The ranges

Table 3 Lingocellulosic SCB compositions (% dry basis)

Biomass	Cellulose	Xylan	Lignin	Other[a]
Sugarcane bagasse	40.50	21.20	24.20	14.1

[a] Ash, non-structural sugars

and levels of independent variables (pH, initial concentration, and adsorbent dosage) are shown in Table 4. The removal percentage of arsenic (As) from aqueous solution was calculated using Eq. (1) as follows:

$$\text{Removal}(\%) = \frac{(C0 - Ce) \times 100}{C0} \quad (1)$$

Where C_0 is the initial arsenic concentration (mg/L), and C_e is the residual or final concentration of arsenic (mg/L).

2.4 Experimental Design and Optimization by RSM

RSM is one of the tools for modeling the experimental processes. This method is based on the statistical analysis of regression consisting of determining an optimal model which minimizes the residual variations. RSM was initially developed for the purpose of determining optimum operation conditions in the chemical industry, but it is now used in a variety of fields and applications not only in the physical and engineering sciences but also in biological, clinical, and social sciences. The response surface design was used in this study to (1) find how jar tests comprising of several levels of arsenic removal factors can be simplified, (2) determine how removal efficiencies (as responses) are affected by changes in the level of adsorbent dose and pH and initial concentration of arsenic (as factors), (3) determine the optimum combination of adsorbent dose, initial concentration, and pH that yields the best removal of arsenic (Trinh and Kang 2010). The Box–Behnken designed experiment model was used for the design of the required number of experiments. Box–Behnken design is devised by George E. P. Box and Donald Behnken as the experimental design in response surface methodology (Myers and Montgomery 2002). Box–Behnken design was used because it was highly efficient, and this design along with RSM was widely applied for the optimization of various physical, chemical, and biological processes (Zhang et al. 2010; Wang et al. 2011). The pH, initial concentration, and adsorbent dosage were considered as effective parameters in adsorption processes. The combined effect of these three factors on arsenic removal was investigated through 17 sets of experiments. The three selected experimental parameters were optimized using RSM considering them as independent variables and percent arsenic removal as response variables. RSM finally fitted the outcomes with an empirical quadratic polynomial model expressed in Eq. 2:

$$Y = \beta_0 + \beta_1 A + \beta_2 B + \beta_3 C + \beta_{11} A^2 + \beta_{22} B^2 + \beta_{33} C^2 + \beta_{12} \text{AB} + \beta_{23} \text{BC} + \beta_{31} \text{CA} \quad (2)$$

Where Y denotes the response variable; β_0 the intercept; β_1, β_2, β_3 the coefficients of the independent variables; β_{11}, β_{22}, β_{33} the quadratic coefficients; β_{12}, β_{23}, β_{31} the interaction coefficients; and A, B, C the independent variables. The variables in this experiment were the adsorbent dosage (A), arsenic initial concentration (B), and pH (C). A positive and a negative sign in the equation show a synergistic effect of the variable and an opposite effect of the variable, respectively. Multivariate regression analysis and optimization process are performed by means of RSM using Design Expert software (version 7.0.0, Stat Ease Inc., USA).

Table 4 The levels and ranges of variables in Box–Behnken statistical experimental design

Independent variables	Symbol	Coded variable level		
		Low −1	Center 0	High +1
Adsorbent dosage (g/L)	A	5	15	25
Arsenic initial concentration (ppm)	B	55	65	75
pH	C	5	7	9

2.5 Kinetics Test

For kinetics study, 1.5 g of adsorbents was added to eight flasks containing 100 mL of polluted water with arsenic. The initial concentration of arsenic was 55 mg/L. The containers were mixed using a mechanical shaker at a speed of 180 rpm at room temperature (24±2 °C). The samples were taken in 15, 30, 45, 60, 90, 120, 150, and 180 min and filtered through a 0.45-μm filter. The filtrate was analyzed for arsenic.

2.6 Adsorption Isotherm Test

It is important to compare sorption performance under the same pH since isotherms could vary with pH, so we conducted our test at pH=9 for SCB and at pH=7 for AC. Different dosages of adsorbents (0.1, 0.5, 1, 1.5 g) were added to four flasks containing 100 mL of polluted water with arsenic. The initial concentration of arsenic was 75 mg/L. The containers were mixed using a

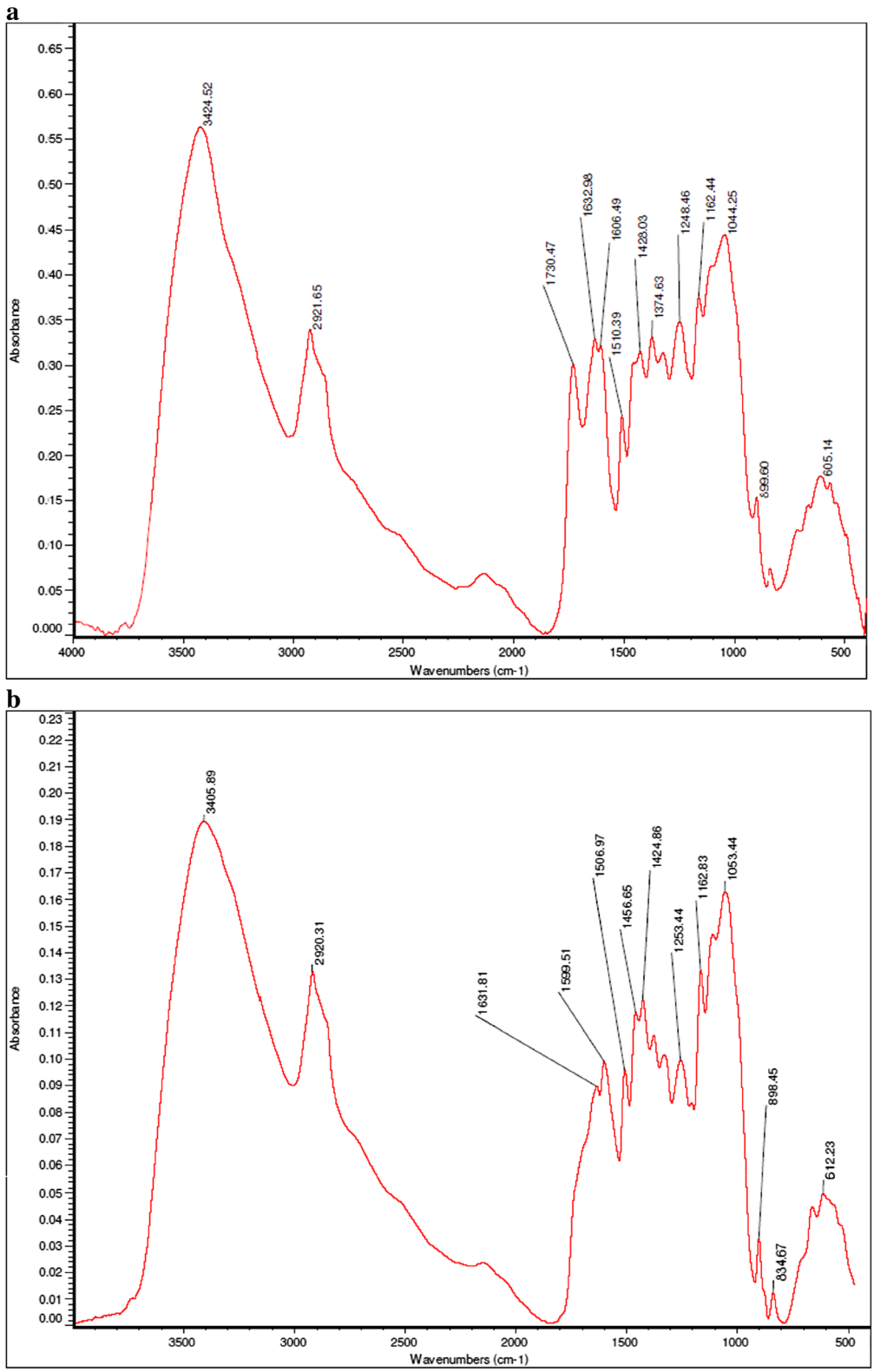

Fig. 1 FTIR spectra of **a** SCB before adsorption process and **b** SCB after adsorption process

mechanical shaker at a speed of 180 rpm at room temperature (24±2 °C).

2.7 Adsorbent Characterization

The determination of the point of zero charge (pH_{pzc}) was conducted to investigate the surface charge of SCB and AC adsorbents. For the determination of pH_{pzc}, 0.1 mol/L of potassium chloride was prepared, and the pH was adjusted between 2 and 12 using diluted hydrochloric acid or sodium hydroxide solution. Then, 50 mL of 0.1 mol/L of potassium chloride solution was placed in a 100-mL conical flask, and 0.1 g of adsorbent was added to each solution. These flasks were kept for 48 h under agitation at room temperature, and the final pH values of the solutions were measured. Graph was plotted between final pH and initial pH. The pH_{pzc} is the point where the final pH versus initial pH curves cross the line equal to pH final (Rivera et al. 2001). Scanning electron microscope (SEM) was used to determine surface morphologies of SCB and AC adsorbents. Properties of the reaction products were characterized by Fourier transform infrared (FTIR) spectra which were obtained with a spectrometer using a pellet (pressure disk) technique, and the analyses were run using the KBr pellet. The spectral range covered was 500–4,000 cm^{-1}.

2.8 Analytical Methods

Arsenic analysis was performed by a Varian (USA) model AA-240 atomic absorption spectrophotometer and pH of solution measured by a pH meter (model of Microprocessor 537). A study of surface characteristics of the adsorbents was conducted using scanning electron microscopy (SEM) (Model Leo, 43SVP) and Fourier transform infrared (FTIR) (Nicolet Model Avatar 370 Csl, Thermo Electron Corporation, USA).

3 Results and Discussions

3.1 Fourier Transform Infrared (FTIR) Spectra Analysis

To understand the chemical change in the structure of SCB before and after the adsorption process, Fourier transform infrared of SCB samples were obtained. Figure 1a, b shows the FTIR spectra of SCB, before and after adsorption processes. The results from FTIR analysis showed the presence of important chemical groups. The most visible differences between the spectra of SCB before and after adsorption processes were found within region 2,000 to 600 cm^{-1}. By comparing the FTIR spectra of treated and original sugarcane bagasse, a broad peak at around 3,400 cm^{-1} represents a broad band of OH groups either from cellulose or lignin. The absorptions of O–H stretching usually occur in a 3,100–3,600 cm^{-1} range (Roberta et al. 1989). The peak at around 2,920 cm^{-1} represents the C–H asymmetric stretching in aliphatic methyl. On the other hand, it could be attributed to CH_2 and CH_3 groups from cellulose, lignin, and hemicellulose. In the case of SCB before adsorption processes, the peaks at 1,606 and 1,510 cm^{-1}, relating to aromatic skeleton vibrations in lignin and the absorption located at 1,730 cm^{-1}, are referred to the acetyl groups which is present in the hemicellulose; this indicates the C=O stretch in non-conjugated ketones, carbonyls, and ester groups. The appearance of the band near 1,600 cm^{-1} is a relative pure ring stretching mode strongly associated with the aromatic C–O–CH3 stretching mode. Band assignments according to the literature and band shifts are listed in Table 5. According to the FTIR spectra of untreated SCB and SCB after adsorption process, the ester bond signal at 1,730 cm^{-1} was reduced after adsorption compared to that of the untreated sample; this suggest that some ester linkages between lignin and carbohydrate were cleaved during adsorption processes. Two small bands at 1,605 and 1,632 cm^{-1} are assigned to the absorbed water and β-glucosidal linkages between the sugar units,

Table 5 Relative absorbance of different groups in Bagasse samples

Assignment of FTIR absorption of sugarcane bagasse	Before adsorption	After adsorption
O–H stretching (H-bonded)	3,424	3,405
C–H cellulose, hemicellulose	1,374	–
C=O stretching carbonyl	1,730	–
O–H vibration of phenolic group	1,248	1,253
O–H stretching of secondary alcohol	1,162	1,162
O–H stretching of primary alcohol	1,044	–
C–H aliphatic axial deformation methyl and methylene groups	2,921	2,920
C–H aliphatic angular deformation CH_2 cellulose, lignin	1,428	1,424; 1,456
C=C aromatic	1,510	1,506
C–Ph vibration	1,606	1,600
C=C aromatic skeletal vibration	1,632	1,631
β-Glycisidic linkages	899	898

respectively. Weak absorptions between 1,500 and 1,400 cm^{-1} arise from the aromatic ring vibrations and ring breathing with C–O stretching in lignin. A band appearing at approximately 1,428 cm^{-1} is due to the bending vibration of C–H of the methylene group. The strong band at 1,162 cm^{-1} in pretreated sugarcane bagasse is assigned to C–O stretching in cellulose, hemicellulose, and lignin or C–O–C stretching in cellulose and hemicelluloses. The band at 896 cm^{-1} is due to glucosidal linkage, peak is at around 899 cm^{-1}, which is due to β-glycosides linkage, which is the same before and after the adsorption process. The peak at 835 cm^{-1} belongs to a C–H out-of-plane vibration in lignin (Owen and Thomas 1989; Hergert 1971; Naser et al. 2010; Bodîrlău and Teacă 2009; Irfan et al. 2011).

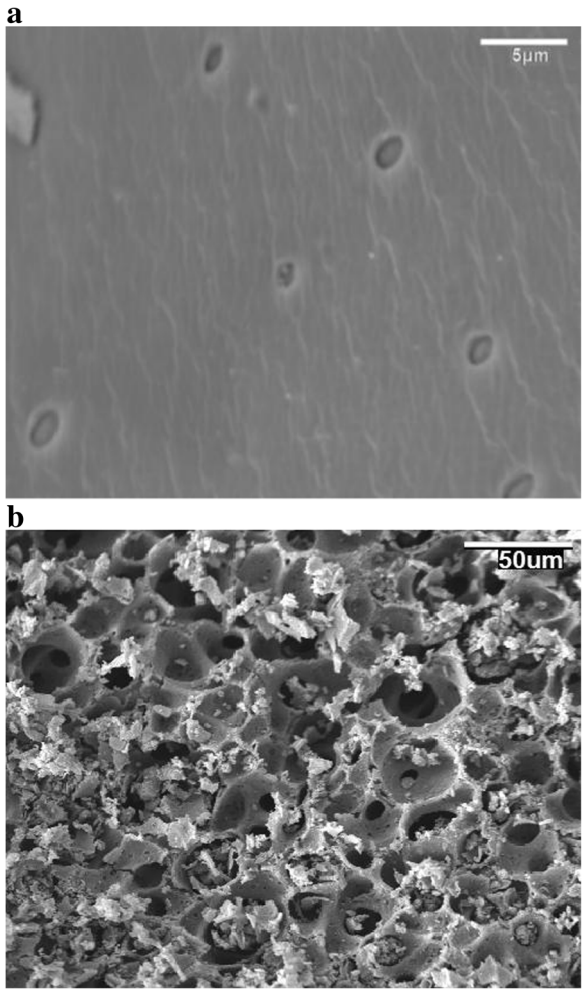

Fig. 2 SEM micrographs of (**a**) the activated carbon (**b**) the sugarcane bagasse

3.2 Scanning Electron Microscope (SEM) Analysis

Scanning electron microscope photos for SCB and AC are presented in Fig. 2a, b. The SEM photograph for AC (Fig. 2a) indicates that large variety of pores is present in AC. It is now generally known that porosity in activated carbons is derived from three main sources, namely the inherent cellular structure of the precursor material, the conditions extant during the preparation of activated carbons, and the composition of the precursor material (Achaw 2012). According to SEM analysis, the microcavities, the main reason for the adsorption power of AC, were detected in its microstructure. Figure 2b shows the presence of fibrous, rough, and irregular surface morphology of SCB. The SEM photographs present the pores of about 1 μm in diameter.

3.3 Statistical Analysis

3.3.1 Model Fitting

A three variable Box–Behnken design was adopted to optimize and investigate the removal of arsenic by AC and SCB. We used this design because it is very efficient and requires minimum number of experiments (Wang

Table 6 Box–Behnken experiments along with actual values of responses

Std	Run	*A*: pH	*B*:C_0 mg/l	C:C_a g/l	Actual value SCB %	Actual value AC %
1	7	5	55	15	62	72
2	17	9	55	15	96.5	83
3	5	5	75	15	69	79
4	13	9	75	15	98	85
5	10	5	65	5	65.3	70
6	16	9	65	5	90	78.6
7	2	5	65	25	60	75
8	9	9	65	25	92.5	84
9	12	7	55	5	62.7	78
10	11	7	75	5	77	75
11	3	7	55	25	68.5	80
12	4	7	75	25	65	86
13	6	7	65	15	79	88.5
14	15	7	65	15	78	88
15	14	7	65	15	77.3	86.5
16	8	7	65	15	78	89
17	1	7	65	15	76.1	88

et al. 2011). In this study, experiments were planned using the Box–Behnken design of RSM to achieve a quadratic model consisting of 12 trials plus five-center points. It is a spherical design containing all points lying on a sphere of a radius square root of two. It does not contain any point on the vertices of the cubic region formed by the upper and lower limits of each variable (Myers and Montgomery 2002; Hergert 1971; Sahoo and Gupa 2012). Table 6 presents the designed experiments by the program with experimental values of the response for AC and SCB. Following the experimental design, the quadratic equations are developed for arsenic removal percentage in terms of the three independent variables as is expressed in Eqs. 3 and 4:

$$\text{COD removal\%(SCB)} = -98.42125 - 11.11000 * \text{pH} + 4.62700 * C_0 + 4.15700 * C_a - 0.068750 * \text{pH} * C_0 + 0.098750 * \text{pH} * C_a - 0.044500 * C_0 * C_a + 1.54625 * \text{pH}2 - 0.024900 * C_0 2 - 0.068900 * C_a 2 \quad (3)$$

$$\text{COD removal\%(AC)} = -141.80000 + 25.57500 * pH + 3.76000 * C_0 + 0.46000 * C_a - 0.062500 * pH * C_0 + 5.00000E{-}003 * pH * C_a + 0.022500 * C_0 * C_a - 1.38750 * pH^2 - 0.027000 * {C_0}^2 - 0.055500 * {C_a}^2 \quad (4)$$

Where, C_a and C_0 are the adsorbent dosages and initial concentration, respectively. The coefficients with one factor (the ones in front of C_a, C_0, and pH) represent the effects of that particular factor, while the coefficients with two factors (the ones in front of C_a * C_0, etc.) and those with second-order terms (the ones in front of ${C_a}^2$, etc.) represent the interaction between the two factors and the quadratic effects. The positive sign in front of the terms indicates a synergistic effect, while the negative sign indicates an antagonistic effect. Consequently, the optimum conditions for the maximum percentage removal of arsenic by AC and SCB were found and shown in Table 7.

3.3.2 Validation of the Models

It is necessary to check the fitted model to ensure its provision to an approximate of the real system adequately. There are some graphical and numerical methods for checking the models. The graphical method characterizes the nature of the residual models. A residual is defined as the difference between an observed value Y and its fitted $\hat{Y}$. The first plot, residuals versus the fitted values (predicted value), as shown in Fig. 3a, was used to test the sufficiency of the functional part of the model. As shown in Fig. 3b, each residual is plotted against an index of observation orders of data which was used to check for any drift in the process. As previously shown in Fig. 3a, b, the graphical residual analysis indicated no obvious pattern, implying that the residuals of the models were randomly distributed. The normal probability plot (scatter diagram) for the studentized residuals is illustrated in Fig. 3c. Points on this plot lie reasonably close to the straight line, confirming that the errors have a normal distribution with a zero mean and a constant value. According to Fig. 3d, the data points were well distributed close to a straight line, which indicated an excellent relationship between the experimental and predicted values of the response for both adsorbents. The results also represented that the chosen quadratic model was appropriate in assuming the response variables for all ranges of the experimental data. The curvature p value <0.0001 indicates that there is a significant curvature (as measured by the difference between the mean center points and the mean factorial points) in the design space. Besides, plots of the residuals in Fig. 1 reveal that they have no obvious pattern and their

Table 7 Optimum conditions selected for the maximum possible COD removal percentage

	No. of solution	*A*, catalytic dose (g/L)	*B*, initial arsenic concentration (ppm)	*C*, pH	Arsenic removal (%)	Desirability
SCB	1	23.68	63.74	8.98	98	1
AC	2	17.55	67.15	7.63	89	1

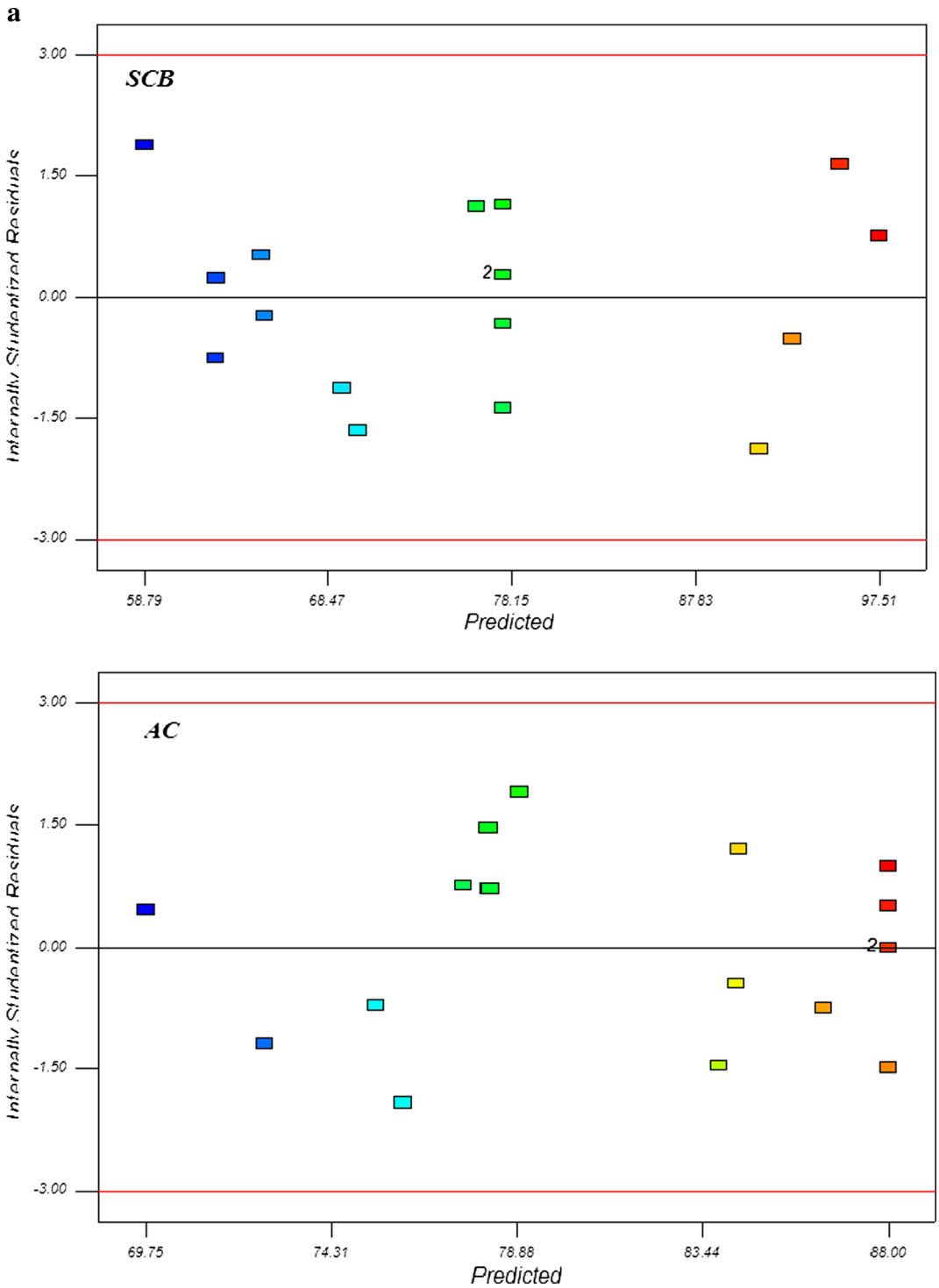

Fig. 3 Statistical analysis plots. **a** Plot of residuals versus the fitted values (predicted value), **b** plot of residual versus order, **c** normal probability plot (scatter diagram), and **d** correlation of actual and predicted values of response for SCB and AC

structure is rather abnormal. Moreover, they indicate equal scatters above and below the *x*-axis, implying the proposed model's adequacy, so there is no reason to suspect any violation (Sahoo and Gupa 2012).

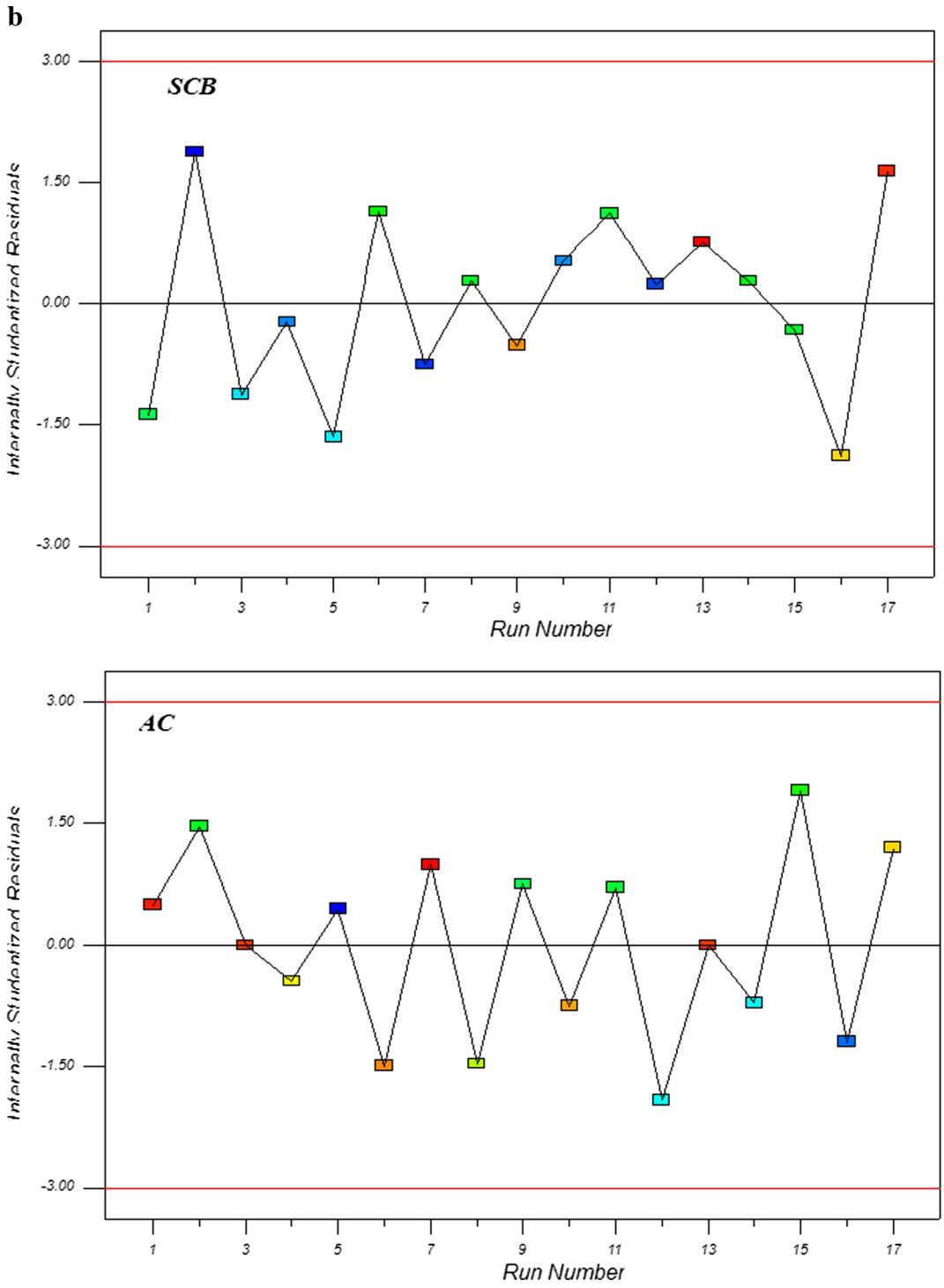

Fig. 3 (continued)

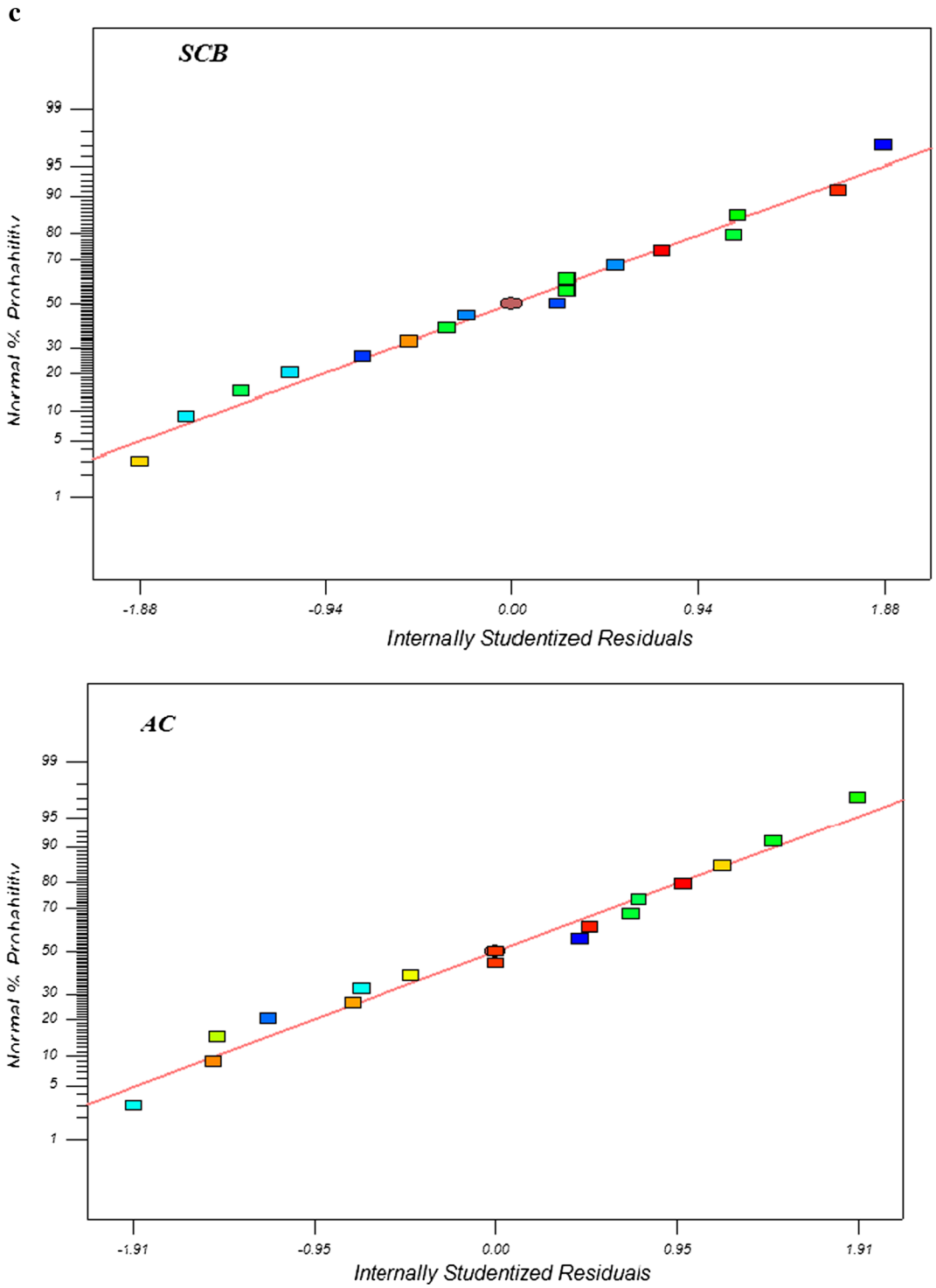

Fig. 3 (continued)

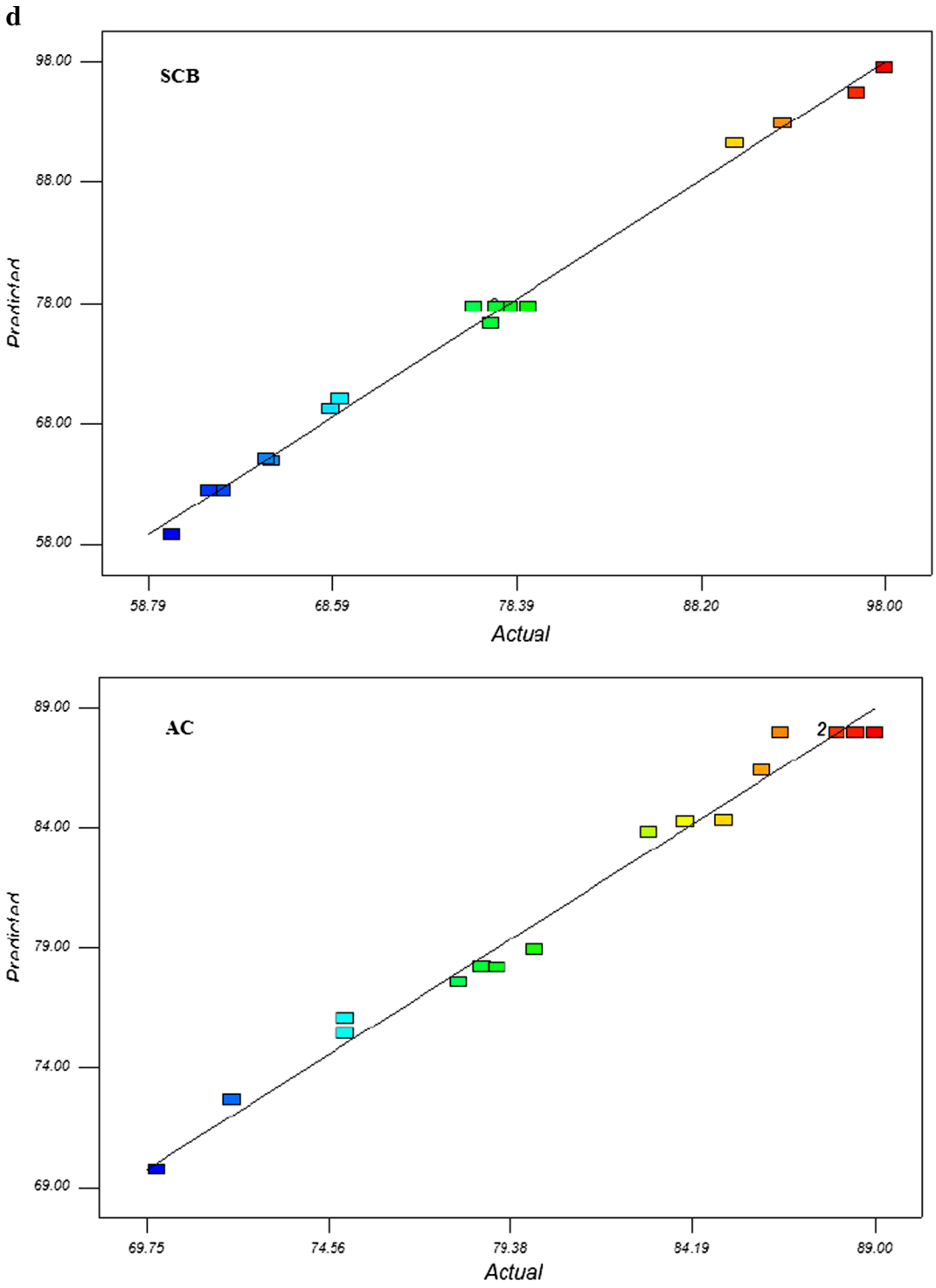

Fig. 3 (continued)

The results were also analyzed by applying the coefficient of determination and then calculated as shown in Eqs. 5 and 6 (Sahoo and Gupa 2012):

$$R^2 = 1 - \frac{\mathrm{SS}_{\mathrm{residual}}}{\mathrm{SS}_{\mathrm{model}} + \mathrm{SS}_{\mathrm{residual}}} \quad (5)$$

$$R^2_{\mathrm{adj}} = 1 - \frac{n-1}{n-p}\left(1 - R^2\right) \quad (6)$$

where SS is the sum of the squares, n the number of experiments, and p the number of predictors (term) in the model, not counting the constant term. To show that the model has good ability to fit the data, higher R^2 predicted and R^2 adjusted are necessary. The more R^2 close to 1, the better the model fits the experimental data. The R^2 for both adsorbents is found to be 0.99, which is close to 1 and significant, this shows that the model can describe about 99 % of the changes in the data.

Table 8 ANOVA for response surface reduced quadratic model—analysis of variance table

Adsorbent type	Source	Sum of squares	DF[a]	Mean square	F value[b]	p value (Prob>F)[c]
SCB	Model	2353.03	9	261.45	157.97	<0.0001*
	A–pH	1062.20	1	1062.20	641.79	<0.0001*
	B–C_0	114.70	1	114.70	69.30	<0.0001*
	C–C_a	92.08	1	92.08	55.64	0.0001*
	AB	7.56	1	7.56	4.57	0.0699*
	AC	15.60	1	15.60	9.43	0.0181*
	BC	79.21	1	79.21	47.86	0.0002*
	A^2	161.07	1	161.07	97.32	<0.0001*
	B^2	26.11	1	26.11	15.77	0.0054**
	C^2	199.88	1	199.88	120.77	<0.0001*
	Residual	11.59	7	1.66	–	–
	Lack-of-fit	7.00	3	2.33	2.03	0.2518**
	Pure error	4.59	4	1.15	–	–
	Cor total	2364.61	16	–	–	–
AC	Model	583.02	9	64.78	51.01	<0.0001*
	A–pH	149.64	1	149.64	117.83	<0.0001*
	B–C_0	18.00	1	18.00	14.17	0.0070*
	C–C_a	68.45	1	68.45	53.89	0.0002*
	AB	6.25	1	6.25	4.92	0.0620**
	AC	0.040	1	0.040	0.031	0.8642**
	BC	20.25	1	20.25	15.94	0.0052*
	A^2	129.69	1	129.69	102.12	<0.0001*
	B^2	30.69	1	30.69	24.17	0.0017*
	C^2	129.69	1	129.69	102.12	<0.0001*
	Residual	8.89	7	1.27	–	–
	Lack-of-fit	5.39	3	1.80	2.05	0.2491**
	Pure error	3.50	4	0.88	–	–
	Cor total	591.91	16	–	–	–

[a] Degree of freedom

[b] Test for comparing model with residual (error) variance

[c] Probability of finding the observed F value when the null hypothesis is true

*Significant at $p<0.05$

**Not significant at $p>0.05$

Analysis of variance (ANOVA) of the regression model was performed to find the significance and interacting effects of parameters on arsenic adsorption procedure. ANOVA table shows the statistical analysis of experimental data for arsenic removal. The results are presented in Table 8. The significance of the coefficient term is proved by values of F and p, and the larger value of F and smaller value of p indicate that most of the variation in the response can be explained by regression equation. The $p<0.05$ indicates that the model is statistically significant. The ANOVA of the quadratic model for both responses (for both adsorbents) indicates that the models are highly significant as the F values for the models are 157.97 for SCB and 51.01 for AC and the

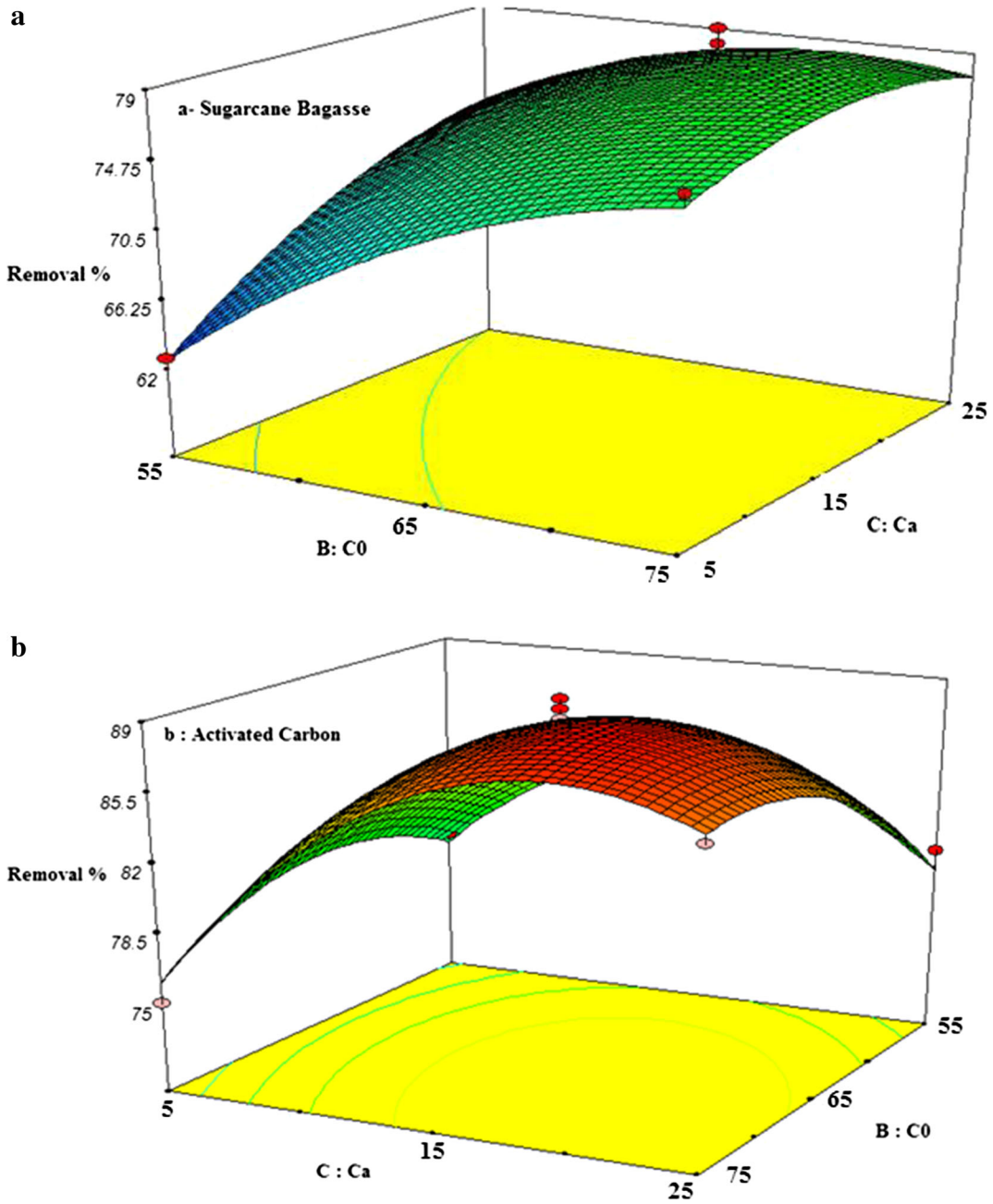

Fig. 4 Three-dimensional response surface plot for the effects of **a** and **b** adsorbent dosage and initial arsenic concentration, **c** and **d** adsorbent dosage and pH, and **e** and **f** initial arsenic concentration and pH on the adsorption of arsenic (As) by SCB and AC

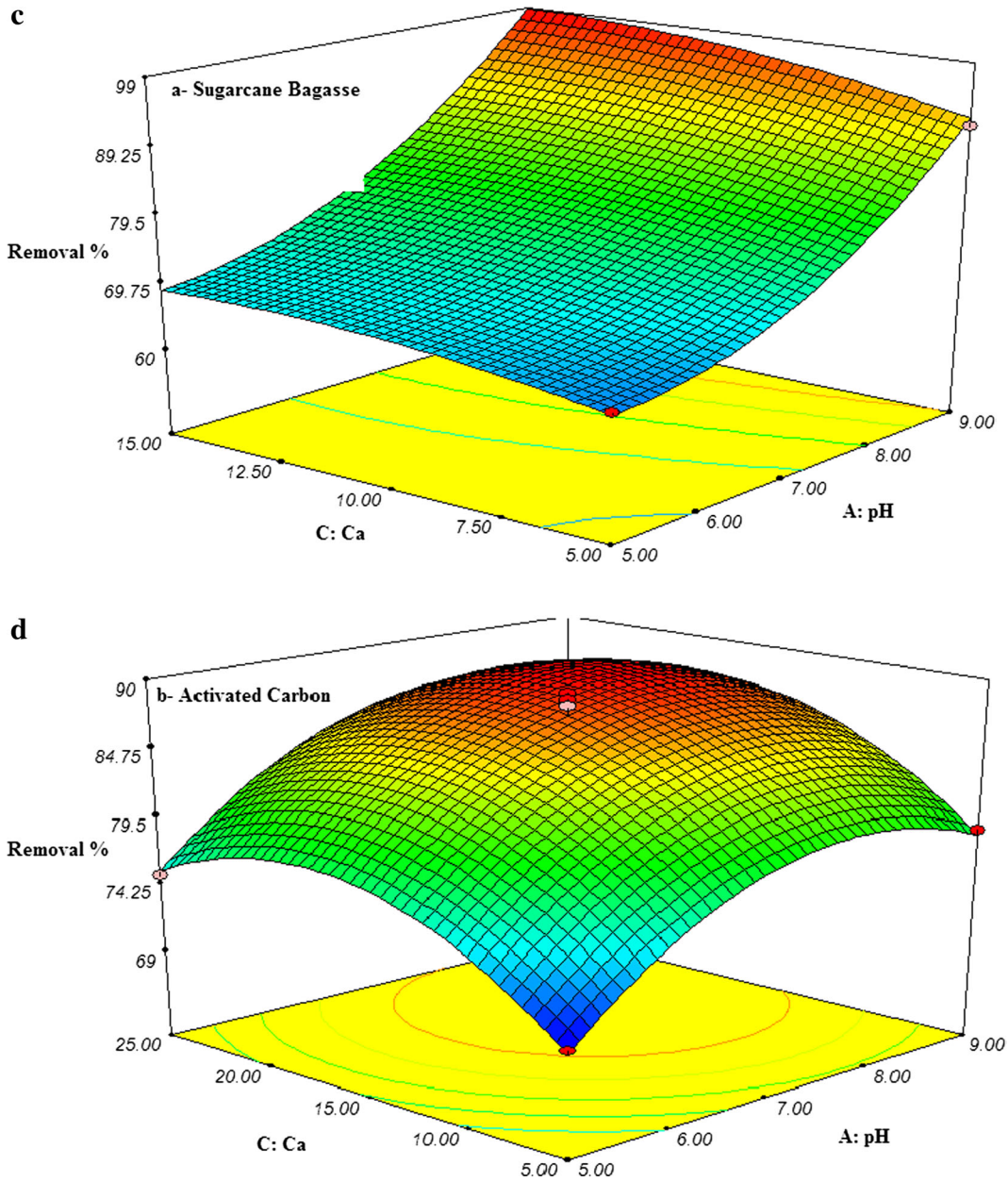

Fig. 4 (continued)

corresponding p values are <0.0001, i.e., there is only a chance of 0.01 % of occurrence of the model's F value due to the noise. The ANOVA regarding the regression models' coefficient of arsenic removal is presented in Table 8 as an extra tool to check the final model's adequacy.

"Adequacy precision" measures the signal to noise ratio. It represents that a ratio greater than 4 is desirable. The ratios of 39.247 and 21.115 for SCB and AC, respectively, show an adequate signal, so this model can be used to navigate the design space. The lack-of-fit p value of 0.2518 for SCB and 0.2491 for AC suggests that the lack-of-fit is not significantly relative to net error; thus, this is desirable since we look for a model that fits.

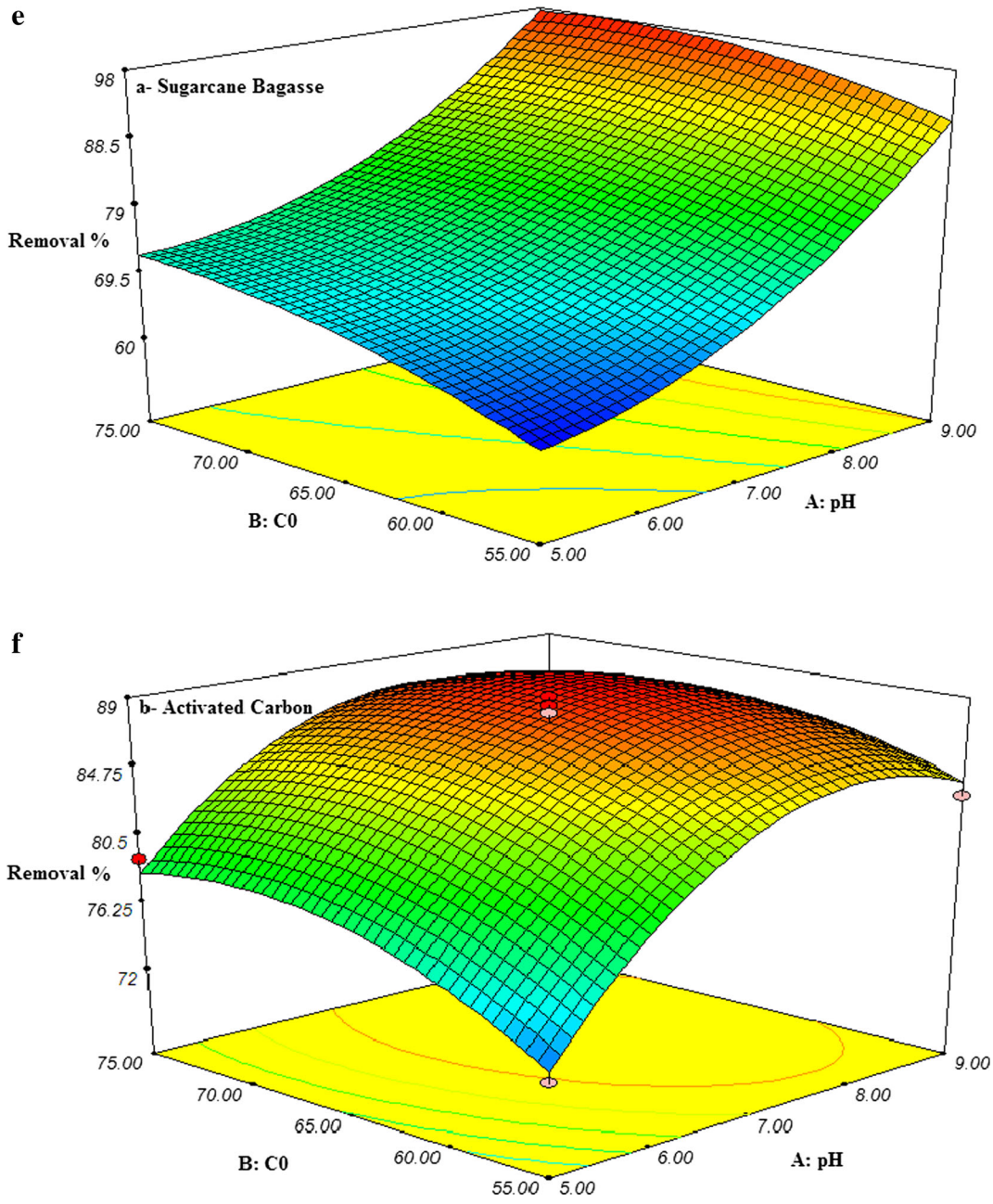

Fig. 4 (continued)

3.4 Effects of Interactive Variables

To determine the adsorption efficiency of arsenic removal from water over interactive variables, 3D surface plot was used. These plots are illustrated in Fig. 4. While the pH of solution was kept constant on 7, the effects of initial arsenic ion concentrations and adsorbent on the adsorption capacity of SCB and AC are shown in Fig. 4a, b, respectively. The maximum arsenic (As) removal of 89 and 98 % were obtained for SCB and AC, respectively. According to Fig. 4a, b, arsenic removal efficiency slightly increased with an increase in the amount of adsorbents, and maximum arsenic (As) removal efficiency was obtained with the adsorbent dosage of 15 g/L for both adsorbents. In the case of AC in the amounts more than 15 g/L, the adsorption

efficiency decreases. The decrease of the adsorption efficiency at a higher dosage of AC may be due to competition among available binding sites. As the amount of AC and SCB increases, the number of surface active sites rises. Increasing the adsorbent dosage provided greater surface area and availability of more metal binding sites; therefore, the rate of arsenic adsorption increased even when the initial arsenic concentration remained constant.

According to Fig. 4a, b, the effect of initial metal ion concentration in the range of 55–75 mg/L on removal efficiency was significantly increasing up to 75 mg/L. At lower arsenic ion concentration, the ratio of the number of moles of arsenic ions in a solution to the available surface area is low; hence, adsorption is independent of the initial concentration. At higher concentration, the number of available sites for adsorption decreases; hence, arsenic removal is dependent on the initial concentration.

While the arsenic ion concentration of solution was kept constant at a value of 55 mg/L, the effects of pH and adsorbent dosage on the adsorption capacity of SCB and AC is shown in Fig. 4c, d.

In general, pH is one of the most important parameters influencing the adsorption process. In the present study, initial pH values of aqueous metal solutions were adjusted from pH 5 to 9, before the addition of the adsorbents. The pH can change the surface properties of adsorbent (AC and SCB). It was found that the removal percentage of arsenic by SCB increased with an increase in pH up to 9, and the optimum pH was found to be 9. In the case of SCB, it was found that the initial pH (7 and 9) had a decrease in the end of experiments, so it is proposed that in these pH levels, arsenite ion is transferred to the surface of SCB, then deprotonation occurs, and finally a surface complex is formed (Wang et al. 2011). H_3AsO_3 is the predominant species for As (III) in the neutral and acid ranges, and neutral molecules were not removed either by adsorption or precipitation onto the positive or neutral surface of the adsorbent so a physical adsorption occurred (Manju et al. 1998).

The nature of the carbon surface was determined from the pH value corresponding to the point of zero charge (pH_{PZC}). In case of AC, The adsorption removal percentage of arsenic was found to increase with an increase in pH up to 7.2, and then it decreased with a further increase of the pH amount. In a case of SCB, the adsorption removal percentage of arsenic was found to increase with an increase in pH up to 9. This behavior is attributed to the changes in the AC and SCB surfaces. The pH $_{PZC}$ of AC and SCB in this study were obtained 7.2 and 10, respectively. When the pH is below pH_{PZC}, the surfaces' charge is predominantly positive; and in pH above the pH $_{PZC}$, negative charges appear on the surface. In the case of As (III) species, however, in acidic pH up to 9, $H_3AsO_3^0$ is the predominant one. Below pH 6, it is only H_3AsO_3. The $H_3AsO_3^0$ is also associated with some amount of $H_2AsO_3^-$ and $H_2AsO_3^{-2}$ in the pH range of 6–9, and the amount of these species increases with an increase in pH (Zhang et al. 2010; Wang et al.2011). It seems that adsorption in this study is a combination of physical and chemical adsorption which high efficiency was obtained.

Experiments for arsenic removal by SCB and AC adsorbents were also performed at different initial metal ion concentrations (55–75 mg/L). The 3D surface plots (Fig. 4e, f) were drawn to depict the effects of initial metal ion concentration (mg/L) and solution pH on arsenic removal efficiency while the adsorbents dosage were kept constant at 15 g/L, being the central level. As

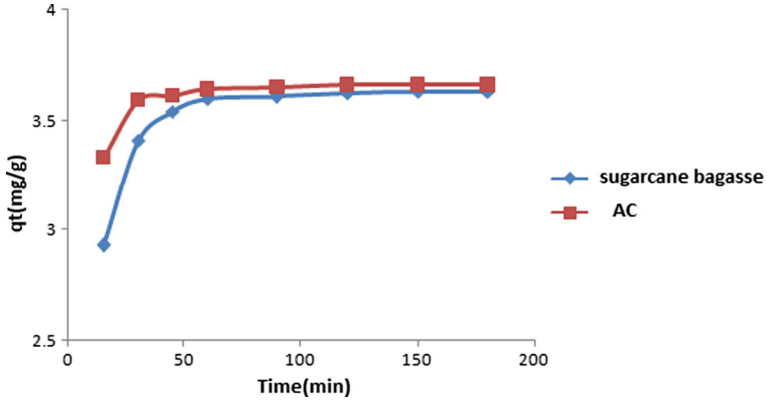

Fig. 5 Effect of contact time on the arsenic adsorption on AC and SCB (temperature=24±2 °C, pH=7 for AC and pH=9 for SCB, dosage=15 g/L, C_0=55 ppm)

Table 9 Estimated kinetic model parameters for arsenic adsorption [a]

	Pseudo-first-order kinetic parameter		Pseudo-second-order kinetic parameter	
	K_1	R_1^2	K^2	R_2^2
SCB	0.06909	0.996	0.07720	0.998
AC	0.07830	0.98	0.269	1

a. *q* adsorbed As (mg/g) at time *t* (min). The initial As addition was 55 mg As/L, and pH was maintained at 9, and absorbent dosage was 15 g/L

shown in Fig. 5e, f, the adsorption potential of SCB and AC was increased by increasing the solution pH from 5 to 9 when metal ion concentration slightly increased from 55 to 75 mg/L.

3.5 Kinetic Studies

In order to obtain kinetic data for arsenic adsorption on the SCB and AC, the time variation of the arsenic concentration was measured. Kinetic study is very important to find out the efficient contact time and

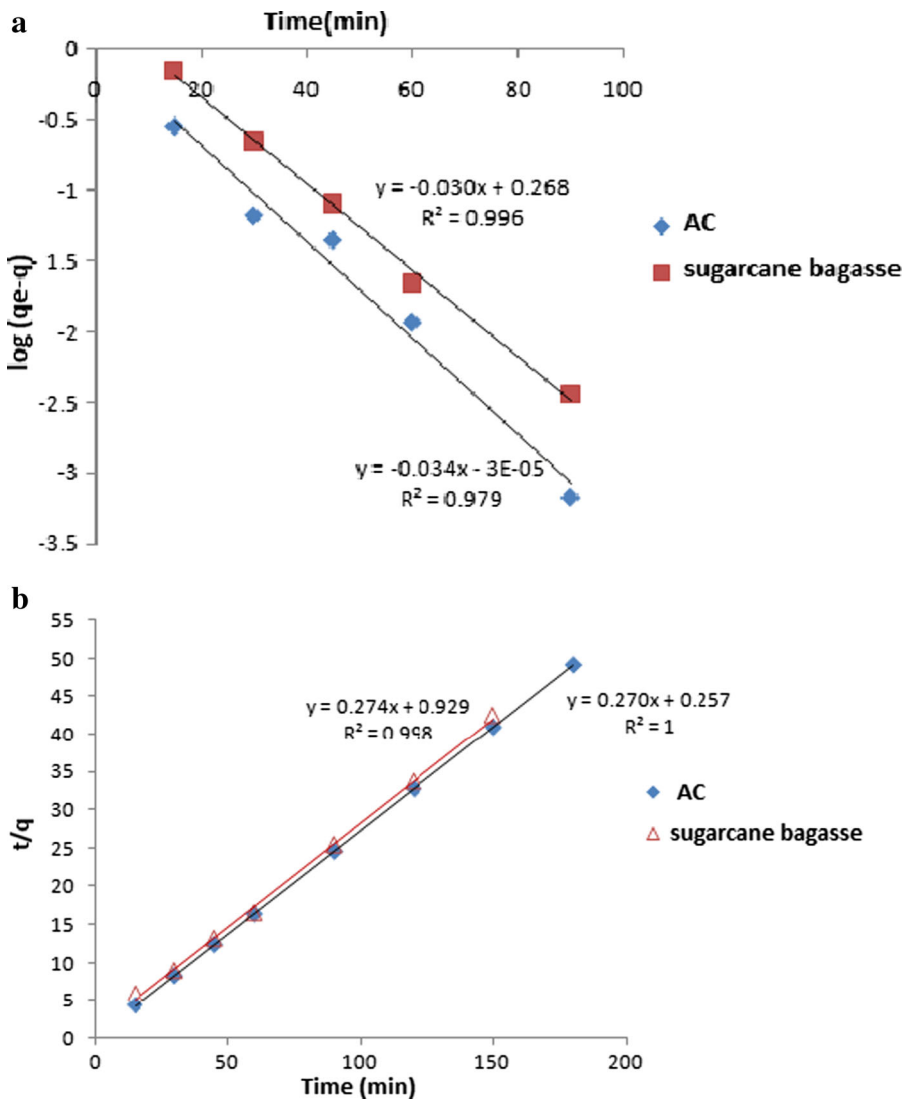

Fig. 6 **a** Pseudo-first-order and **b** pseudo-second-order adsorption kinetic model for arsenic adsorbed on AC and SCB (temperature=24± 2 °C, pH=7 for AC and pH=9 for SCB, dosage=15 g/L, C_0=55 ppm)

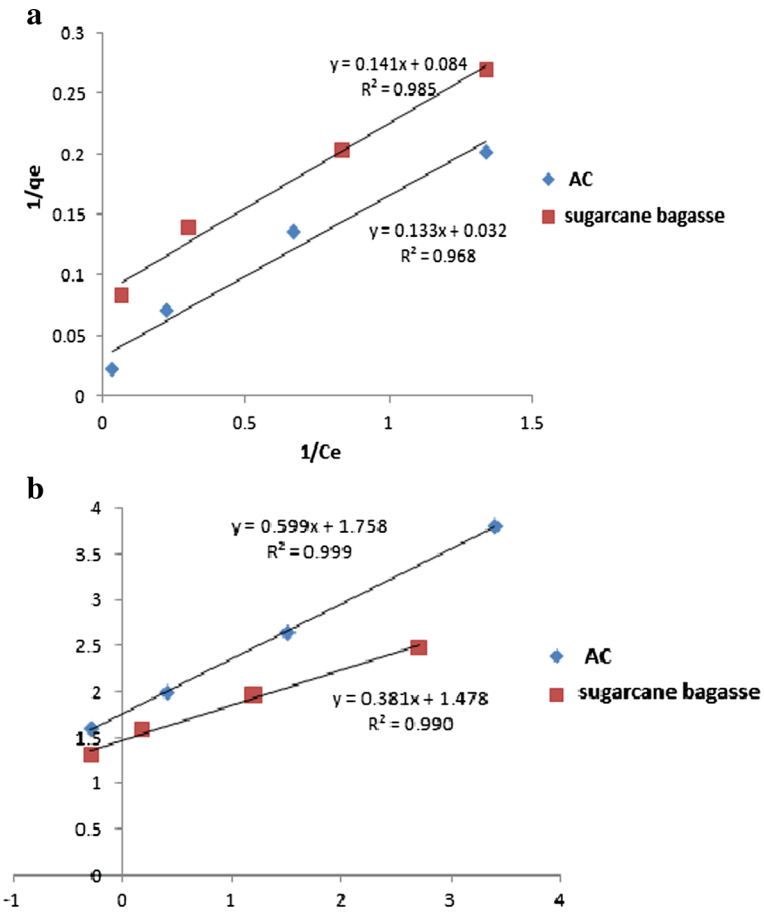

Fig. 7 **a** Langmuir and **b** Freundlich adsorption isotherm for arsenic adsorbed on AC and SCB (initial concentration= 75 ppm, temperature=24±2 °C, pH=7 for AC and pH=9 for SCB, and dosage=1, 5, 10, 15 g/L)

for evaluating reaction coefficients. The rate of arsenic uptake by AC and SCB from aqueous solution is shown in Fig. 5 which indicates that the amount of arsenic adsorption increases with the increase in shaking time; and after certain operating time, it tends to approach a constant value. It was found that the initial adsorption of arsenic was rapid for both AC and SCB. However, arsenic adsorption on SCB was slightly faster than adsorption on AC at a fixed time. The achieved equilibriums were 120 min for SCB and 150 min for AC. Two popular kinetic models, pseudo-first-order and pseudo-second-order, were used to fit the kinetic data by linear regression (Maji et al. 2008; Polowczyk et al. 2010; Biswas et al. 2008). The linear forms of these models can be expressed as follows in Eqs. 7 and 8.

$$\log(q_e - q) = \log q_e - \frac{k_1.t}{2.303} \tag{7}$$

$$\frac{t}{q} = \frac{1}{k_2 q_e^2} + \frac{1}{q_e} t \tag{8}$$

Where k_1 and k_2 are rate constants for the pseudo-first-order (1/min) and the pseudo-second-order adsorption [g/(mg min)], respectively, while q_t and q_e are the amounts of arsenic adsorbed (mg/g) at any time t and at equilibrium, respectively. These model equations and estimated parameters with R^2 and K are tabulated in Table 9. Based on R^2 and K, the kinetics of arsenic adsorption on SCB adsorbent can be best fitted by pseudo-first-order and pseudo-second-order equations

Table 10 Langmuir and Freundlich isotherm constants

Adsorbent	Langmuir isotherm parameters				Freundlich isotherm parameters		
	q_{max}	b	r^2	RL	k	n	r^2
AC	31.25	0.24	0.968	0.052	5.8	1.669	0.99
SCB	11.9	0.59	0.985	0.022	4.4	2.7	0.985

while the pseudo-first-order rate equation did not truly reflect the experimental results. However, the kinetic data for arsenic adsorption on AC could be well fitted by pseudo-second-order equation with a R^2 value ~1. (Fig. 6a, b)

3.6 Adsorption Isotherms

Adsorption isotherms for SCB and AC were shown in Fig. 7a, b, respectively. Langmuir and Freundlich models are used to investigate the maximum adsorption capacity of both AC and sugarcane bagasse. The Freundlich isotherm model assumes a heterogeneous sorption surface and supposes different energies for the active sites. The Langmuir theory assumes that sorption takes place at specific homogeneous sites within the sorbent. It is assumed that no further adsorption can take place in a site when a molecule occupies a site. Consequently, the sorbent has a finite capacity for the sorbets (Lee 2010; Wilpo et al. 2008). The results show that the arsenic adsorption fits well with Langmuir and Freundlich isotherm models (R^2>0.98) for both absorbents. Adsorption constants evaluated from the linearized Langmuir (1918) adsorption isotherm are as follows:

$$\frac{1}{qe} = \frac{1}{qmb}\left(\frac{1}{C_0}\right) + \frac{1}{qm} \tag{9}$$

And the Freundlich (1906) isotherms are the following:

$$Ln(q_e) = Ln(k) + \frac{1}{n} LnC_e \tag{10}$$

Langmuir and Freundlich parameters are listed in Table 10. The q_{max} is the maximum adsorption capacity and can also be explained as the total number of binding sites which are available for adsorption, b is the adsorption constant related to the enthalpy of adsorption. n and k are constants depending upon the nature of adsorption and adsorbent. K indicates the adsorption capacity and the strength of the adsorptive bonds, and n is the heterogeneity factor which represents the bond distribution and adsorption intensity and varies with the heterogeneity of the material. The heterogeneity factor describes reversible adsorption and is not restricted to the formation of the monolayer (Al-Khatib et al. 2012). Arsenic adsorption capacity was ~35.25 mg/g and 11.9 mg/g for AC and SCB, respectively. These are in the range of the adsorption capacity of most reported adsorbents (Di Natale et al. 2008; Budinova et al. 2009; Zhu et al. 2009).

Adsorption type can be evaluated by R_L as follows (Hall et al. 1966):

$$R_L = \frac{1}{1 + b \times C_0} \tag{11}$$

In this study, R_L lies in the range of 0 to 1, for both AC and SCB, which infers a favorable adsorption of arsenic at the studied conditions.

4 Conclusions

In general, most types of AC have high ability for arsenic and other toxic material removal from water. The SCB has good removal efficiency for As (III) aqueous solution with 98 % sorption efficiency of 65 mg/L As (III) solution by 25 g/L adsorbent dosage at pH=9. In the case of AC, the maximum efficiency was obtained at pH=7. Arsenic adsorption on bagasse was slightly faster than adsorption on AC at a fixed time. The equilibrium time was 120 min for SCB and 150 min for AC. Isotherm studies showed that arsenic adsorption capacity was ~35.25 and 11.9 mg/g for AC and SCB, respectively. As a result, SCB is an efficient low-cost biosorbent for arsenic removal from water and can be a good alternative for synthetic adsorbent material suchas AC.

References

Achaw, O. W. (2012). A study of the porosity of activated carbons using the scanning electron microscope, Scanning electron microscopy, Dr. Viacheslav Kazmiruk (Ed.), ISBN: 978-953-51-0092-8, InTech.

Akhtar, M., Hasany, S. M., Bhanger, M. I., & Iqbal, S. (2007). Low cost sorbents for the removal of methyl parathion pesticide from aqueous solutions. *Chemosphere, 66*, 1829–1838.

Akhter, H., Cartledge, F. K., Roy, A., & Tittlebaum, M. E. (1997). Solidification/stabilization of arsenic salts: effects of long cure times. *Journal of Hazardous Materials, 52*, 247–264.

Al-Khatib, L., Fraige, F., Al-Hwaiti, M., & Al-Khashman, O. (2012). Adsorption from aqueous solution onto natural and acid activated bentonite. *American Journal of Environmental Science, 8*, 510–522.

Altundogan, H. S., Altundogan, S., Tumen, F., & Bildik, M. (2002). Arsenic adsorption from aqueous solutions by activated red mud. *Waste Management, 22*, 357–363.

Amin, M. N., Kaneco, S., Kitagawa, T., Aleya, B., Katsumata, H., Suzuki, T., et al. (2006). Removal of arsenic in aqueous solutions by adsorption onto waste rice husk. *Industrial and Engineering Chemistry Research, 45*, 8105–8110.

Ayyappan, R., Sophia, C. A., Swaminathan, K., & Sandhya, S. (2005). Removal of Pb(II) from aqueous solution using carbon derived from agricultural wastes. *Process Biochemistry, 40*, 1293–1299.

Baskan, M. B., & Pala, A. (2011). Removal of arsenic from drinking water using modified natural zeolite. *Desalination, 281*, 396–403.

Biswas, B. K., Inoue, J., Inoue, K., Kedar Nath, G., Harada, H., Ohto, K., et al. (2008). Adsorptive removal of As(V) and As(III) from water by a Zr(IV)-loaded orange waste gel. *Journal of Hazardous Materials, 154*, 1066–1074.

Bodîrlău, R., & Teacă, C. A. (2009). Fourier transform infrared spectroscopy and thermal analysis of lignocellulose fillers treated with organic anhydrides. *Romanian Journal of Physiology, 54*(1–2), 93–104.

Budinova, T., Petrov, N., Razvigorova, M., Parra, J., & Galiatsatou, P. (2006). Removal of arsenic(III) from aqueous solution by activated carbons prepared from solvent extracted olive pulp and olive stones. *Industrial and Engineering Chemistry Research, 45*, 1896–1901.

Budinova, T., Savova, D., Tsyntsarski, B., Ania, C. O., Cabal, B., Parra, J. B., et al. (2009). Biomass waste-derived activated carbon for the removal of arsenic and manganese ions from aqueous solutions. *Applied Surface Science, 255*, 4650–4657.

Cristina, R., Corrales, N. R., Magalhães, F., Mendes, T., Cruz Perrone, C., et al. (1989). Structural evaluation of sugar cane bagasse steam pretreated in the presence of CO_2 and SO_2, N.L. Owen, D.W. Thomas, Infrared studies of "hard" and "soft" woods. *Applied Spectroscopy, 43*, 451–455.

Di Natale, F., Erto, A., Lancia, A., & Musmarra, D. (2008). Experimental and modelling analysis of As(V) ions adsorption on granular activated carbon. *Water Research, 42*, 2007–2016.

Eljamal, O., Sasaki, K., & Hirajima, T. (2011). Numerical simulation for reactive solute transport of arsenicin permeable reactive barrier column including zero-valent iron. *Applied Mathematical Modelling, 35*, 5198–5207.

Freundlich, H. (1906). Adsorption solution. *Zeitschrift für Physikalische Chemie, 57*, 384–470.

Garg, U., Kaur, M. P., Jawa, G. K., Sud, D., & Garg, V. K. (2008). Removal of cadmium(II) from aqueous solutions by adsorption on agriculture waste biomass. *Journal of Hazardous Materials, 154*, 1149–1157.

Gupta, V. K., & Ali, I. (2000). Utilization of bagasse fly ash (a sugar industry waste) for the removal of copper and zinc from wastewater. *Separation and Purification Technology, 18*, 131–140.

Gupta, V. K., & Ali, I. (2001). Removal of DDD and DDE from wastewater using bagasse fly ash, a sugar industry waste. *Water Research, 35*(1), 33–40.

Gupta, V. K., & Ali, I. (2004). Removal of lead and chromium from wastewater using bagasse fly ash—a sugar industry waste. *Journal of Colloid and Interface Science, 271*, 321–328.

Gupta, V. K., Mohan, D., & Sharma, S. (1998a). Removal of lead from wastewater using bagasse fly ash—a sugar industry waste material. *Separation Science and Technology, 33*(9), 1331–1343.

Gupta, V. K., Sharma, S., Yadava, I. S., & Mohan, D. (1998b). Utilization of bagasse fly ash generated in sugar industry for the removal and recovery of phenol and *p*-nitrophenol from wastewater. *Journal of Chemical Technology and Biotechnology, 71*, 180–186.

Gupta, V. K., Mohan, D., Sharma, S., & Park, K. T. (1999). Removal of chromium(VI) from electroplating industry wastewater using bagasse fly ash—a sugar industry waste material. *Environmentalist, 19*(2), 129–136.

Gupta, V. K., Mohan, D., Sharma, S., & Sharma, M. (2000). Removal of basic dyes (rhodamine-B and methylene blue) from aqueous solutions using bagasse fly ash. *Separation Science and Technology, 35*(13), 2097–2113.

Gupta, V. K., Jain, C. K., Ali, I., Sharma, M., & Saini, V. K. (2003). Removal of cadmium and nickel from waste water using bagasse fly ash—a sugar industry waste. *Water Research, 37*, 4038–4044.

Gupta, V. K., Ali, I., Saini, V. K., Gerven, T. V., Bruggen, B. V., & Vandecasteele, C. (2005). Removal of dyes from wastewater using bottom ash. *Industrial and Engineering Chemistry Research, 44*(11), 3655–3664.

Gupta, V. K., Ali, I., Suhas, J. S., & Saini, V. K. (2006). Adsorption of 2,4-d and carbofuran pesticides using fertilizer and steel industry wastes. *Journal of Colloid and Interface Science, 299*(2), 556–563.

Gupta, V. K., Carrott, P. J. M., Ribeiro Carrott, M. M. L., & Suhas, J. S. (2009). Low cost adsorbents: growing approach to wastewater treatment—a review. *Critical Reviews in Environmental Science and Technology, 39*, 783–842.

Hall, K. R., Eagleton, L. C., Acrivos, A., & Vermeulen, T. (1966). Pore- and solid-diffusion kinetics in fixed-bed adsorption under constant-pattern conditions. *Industrial and Engineering Chemistry Fundamentals, 5*, 212–223. doi:10.1021/i160018a011.

Hergert, H. L. (1971). Infrared spectra. In K. V. Sarkanen & C. H. Ludwig (Eds.), *Lignin: occurrence* (pp. 267–297). New York: Formation, Structure and Reactions, Wiley.

Irfan, M., Syed, Q., Abbas, S., Sher, M. G., Baig, S., & Nadeem, M. (2011). FTIR and SEM analysis of thermo-chemical fractionated sugarcane bagasse. *Turkish Journal of Biochemistry-Turkish Journal of Biochemistry, 36*(4), 322–328.

Kamala, C. T., Chu, K. H., Chary, N. S., Pandey, P. K., Rameshd, S. L., Sastry, A. R. K., et al. (2005). Removal of arsenic (III) from aqueous solutions using fresh and immobilized plant biomass. *Water Research, 39*, 2815–2826.

Khoramzadeh, E., Nasernejad, B., & Halladj, R. (2013). Mercury biosorption from aqueous solutions by sugarcane bagasse. *Journal of Taiwan Institute of Chemical Engineers, 44*, 266–269.

Ladeira, A. C. Q., & Ciminelli, V. S. T. (2004). Adsorption and desorption of arsenic on an oxisol and its constituents. *Water Research, 38*(8), 2087–2094.

Langmuir, I. (1918). The adsorption of gases on plane surfaces of glass, mica and platinum. *Journal of the American Chemical Society, 40*, 1361–1403. doi:10.1021/ja02242a004.

Lee, S. (2010). Application of activated carbon fiber (ACF) for arsenic removal in aqueous solution. *Korean Journal of Chemical Engineering, 27*, 110–115.

Maiti, A., Sharma, H., Basu, J. K., & De, S. (2009). Modeling of arsenic adsorption kinetics of synthetic and contaminated groundwater on natural laterite. *Journal of Hazardous Materials, 117*, 928–934.

Maji, S. K., Pal, A., & Pal, T. (2008). Arsenic removal from real-life groundwater by adsorption on laterite soil. *Journal of Hazardous Materials, 151*, 811–820.

Mane, V. S., Mall, I. D., & Srivastava, V. C. (2007). Use of bagasse fly ash as an adsorbent for the removal of brilliant green dye from aqueous solution. *Dyes and Pigments, 73*, 269–278.

Manju, G. N., Raji, C., & Anirudhan, T. S. (1998). Evaluation of coconut husk carbon for the removal of arsenic from water. *Water Research, 32*(10), 3062–3070.

Mohan, D., & Pitmann, C. U., Jr. (2007). Arsenic removal from water/wastewater using adsorbents—a critical review. *Journal of Hazardous Materials, 142*, 1–53.

Mohan, D., & Singh, K. P. (2002). Single and multi-component adsorption of cadmium and zinc using activated carbon derived from bagasse—an agricultural waste. *Water Research, 36*, 2304–2318.

Murugesan, G. S., Sathishkumar, M., & Swaminathan, K. (2006). Arsenic removal from groundwater by pretreated waste tea fungal biomass. *Bioresource Technology, 97*, 483–487.

Myers, R. H., & Montgomery, D. C. (2002). *Response surface methodology: process and product optimization using designed experiments* (2nd ed.). USA: John Wiley and Sons.

Nasar, M., Emam, A., Sultan, M., & Abdel Hakim, A. A. (2010). Optimization and characterization of sugar-cane bagasse liquefaction process. *Indian Journal of Science and Technology, 3*(2), 0974–6846.

Owen, N. L., & Thomas, D. W. (1989). Infrared studies of "hard" and "soft" woods, Appl. *Spectroscopy 43*, 451–455

Pandey, P. K., Choubey, S., Verma, Y., Pandey, M., & Chandrashekhar, K. (2009). Biosorptive removal of arsenic from drinking water. *Bioresource Technology, 100*, 634–637.

Pattanayak, J., Mondal, K., Mathew, S., & Lalvani, S. B. (2000). A parametric evaluation of the removal of As(V) and As(III) by carbon based adsorbents. *Carbon, 38*, 589–596.

Polowczyk, I., Bastrzyk, A., Koźlecki, T., Sawiński, W., Rudnicki, P., Sokołowski, A., et al. (2010). Use of fly ash agglomerates for removal of arsenic. *Environmental Geochemistry and Health, 32*, 361–366.

Rao, M., Parwate, A. V., & Bhole, A. G. (2002). Removal of Cr6+ and Ni2+ from aqueous solution using bagasse and fly ash. *Waste Management, 22*, 821–830.

Rao, M. M., Reddy, D. H. K. K., Venkateswarlu, P., & Seshaiah, K. (2009). Removal of mercury from aqueous solutions using activated carbon prepared from agricultural by-product/waste. *Journal of Environmental Management, 90*, 634–643.

Rivera-Utrilla, J., Bautista-Toledo, I., Ferro- Garcy, M. A., & Moreno, C. (2001). Activated 1 carbon surface modifications by adsorption of bacteria and their effect on aqueous lead adsorption. *Journal of Chemical Technology and Biotechnology, 76*, 1209–1215.

Sahoo, C., & Gupta, A. K. (2012). Optimization of photocatalytic degradation of methyl blue using silver ion doped titanium dioxide by combination of experimental design and response surface approach. *Journal of Hazardous Materials, 215–216*, 302–310.

Sari, A., Uluozlü, Ö. D., & Tüzen, M. (2011). Equilibrium, thermodynamic and kinetic investigations on biosorption of arsenic from aqueous solution by algae (*Maugeotia genuflexa*) biomass. *Separation Science and Technology, 167*, 155–161.

Srivastava, S. K., Gupta, V. K., Johri, N., & Mohan, D. (1995a). Removal of 2,4,6-trinitrophenol using bagasse fly ash—a sugar industry waste material. *Indian Journal of Chemical Technology, 2*, 333–336.

Srivastava, S. K., Gupta, V. K., Yadava, I. S., & Mohan, D. (1995b). Removal of 2,4-dinitrophenol using bagasse fly ash—a sugar industry waste material. *Fresenius Environmental Bulletin, 4*, 550–557.

Trinh, T. K., & Kang, L. S. (2010). Application of response surface method as an experimental design to optimize coagulation tests. *Environmental Engineering Research, 15*, 063–070.

Urík, M., Littera, P., Ševc, J., Kolenčík, M., & Čerňanský, S. (2009). Removal of arsenic (V) from aqueous solutions using chemically modified sawdust of spruce (Picea abies): kinetics and isotherm studies. *International Journal of Environmental Science and Technology, 6*, 451–456.

Wang, J. P., Chen, Y. Z., Wang, Y., Yuan, S. J., & Yu, H. Q. (2011). Optimization of the coagulation–flocculation process for pulp mill wastewater treatment using a combination of uniform design and response surface methodology. *Water Research, 45*, 5633–5640.

Wilopo, W., Sasaki, K., Hirajima, T., & Yamanaka, T. (2008). Immobilization of arsenic and manganese in contaminated groundwater by permeable reactive barriers using zero valent iron and sheep manure. *Materials Transactions, 49*, 2265–2274.

Zhang, J., Fu, D., Xu, Y., & Liu, C. (2010). Optimization of parameters on photocatalytic degradation of chloramphenicol using TiO2 photocatalyst by response surface methodology. *Journal of Environmental Sciences, 22*, 1281–1289.

Zhu, H., Jia, Y., Wu, X., & Wang, H. (2009). 106. Removal of arsenic from water by supported nano zero-valent iron on activated carbon. *Journal of Hazardous Materials, 172*, 1591–1596.